Digital Innovations & Contemporary Research in SCIENCE, ENGINEERING & TECHNOLOGY
Vol. 10. No. 3, September 2022

Article Citation Format
Adeyemo, I. A., Ojo, J. A.. & Adegbola, O. A. (2022): Selective Harmonic Elimination in Standalone Single-Phase Multilevel Inverter Connected to Photovoltaic Array. Journal of Digital Innovations & Contemporary Research in Science, Engineering & Tech. Vol. 10, No. 3. Pp 121-136

Article Progress Time Stamps
Article Type: Research Article
Manuscript Received: 12th June, 2022
Review Type: Blind
Final Acceptance: 28th August, 2022

Selective Harmonic Elimination in Standalone Single-Phase Multilevel Inverter Connected to Photovoltaic Array

Adeyemo, I. A.[1], Ojo, J. A.[2]. & Adegbola, O. A.[3]
[1, 2, 3]Department of Electronic & Electrical Engineering
Ladoke Akintola University of Technology
PMB 4000, Ogbomoso, Oyo State, Nigeria.
Emails: iaadeyemo@lautech.edu.ng, jaojo@lautech.edu.ng, oaadegbola@lautech.edu.ng

ABSTRACT

The advent of high-speed semiconductor switches with high-power handling capability has led to the widespread use of renewable energy based distributed power generation in remote and rural locations. In this study, a photovoltaic (PV) system based 11-level cascaded H-bridge (CHB) inverter is presented for single-phase applications in off grid locations. Each of the five H-bridges in the 11-level CHB inverter is powered by a separate 1 kW PV array-connected DC-DC boost converter. The PV generated voltage, which varies with temperature and irradiance is regulated and stepped up with the DC-DC boost converter. The regulated DC voltage, which is the DC link voltage required for the operation of each H-bridge in the DC-AC multilevel inverter is maintained at the maximum power point value using perturb and observe maximum power point tracking (MPPT) algorithm. By solving a set of transcendental nonlinear selective harmonic elimination (SHE) equations with Newton Raphson iterative method, selective harmonic elimination pulse width modulation (SHEPWM) technique is deployed for the elimination of the lower order harmonics specifically 3rd, 5th, 7th and 9th harmonics in the 11-level single-phase CHB inverter. The viability of the proposed PV system based multilevel inverter is demonstrated with simulations in MATLAB/SIMULINK environment. Computational results are validated with simulation results with both results in close agreement.

Keywords - Boost converter, harmonics, multilevel inverter, MPPT, and PV array.

1. INTRODUCTION

Sequel to the unabating increase in the global power demand and the high costs associated with the extensions of the power grid system to remote and rural locations, the electric power generation, transmission and distribution are experiencing dramatic changes. There is now a paradigm shift from the traditional power system in which centralized fossil fuel power plants and the load centres are connected by long transmission lines to the on-site distributed power generation from sources of energy that are renewable and sustainable.

Distributed power system includes arrays of solar photovoltaic panels, wind farms, hydroelectric, biomass and tidal power plants. Among distributed power generation schemes, wind farms and solar technology are the most promising schemes, even envisaged as competing with the traditional fossil fuel power plants in the near future [1].

The increasing share of renewable energy sources in power generation is attributable to the challenges experienced with the traditional power generation such as dwindling supply of fossil fuel, climate change caused by emission of greenhouse gasses and high cost that is incurred in the extensions of the power grid system to remote and rural locations. These challenges led to a quest for alternatives to conventional power generation schemes that are not only able to meet the increasing power demand but also ensure that power quality standards such as IEEE 519-1992 and IEC61000-3-12 are met as well [2].

Power electronic converters have been recognized in the distribution generation system as the core enabling technology for harnessing renewable energy. DC- to - AC power electronic converters are known as inverters. Generally, there are three types of inverters namely Z-source inverter [3], voltage source inverter (VSI) and current source inverter (CSI) [4]. Voltage source inverters, which synthesize an output AC voltage of desired magnitude and frequency from a slowly varying DC input voltage are broadly classified into four categories according to their output waveforms: square wave, modified square wave (also called quasi-square or modified sine wave), multilevel (or multi-step) and sine wave [5]. Although both square wave and the modified sine wave inverters are acceptable in some practical applications and are still available in the market, their major drawback is high harmonic content [5]. The major difference between multilevel inverters and sine wave inverters is the switching frequency [5], [6]. Multilevel inverter is based on low frequency switching while sine wave inverter is based on high frequency switching. Fast switching in pure sine inverter results in high switching losses thus reducing the inverter efficiency [6].

The advent of high-speed and high-power semiconductor switches coupled with intensive research activities in the field of power electronic conversion have resulted in the extension of traditional two-level modulation techniques to several levels. Multilevel inverter modulation techniques include sinusoidal pulse width modulation (SPWM), space vector modulation (SVM), and selective harmonics elimination pulse width modulation (SHEPWM) [7], [8]. Compared with the other multilevel inverter modulation techniques, SHEPWM technique arguably gives the highest quality output. SHEPWM technique at fundamental switching frequency has many advantages among which are; high-quality output spectra, low switching losses and the direct control of harmonics. In SHEPWM technique, specified low order harmonics are eliminated or minimized by solving a set of nonlinear and transcendental equations known as selective harmonic elimination (SHE) equations that characterize the targeted harmonics, while the fundamental harmonic is satisfied [7], [8]. The main challenge associated with SHEPWM technique is the heavy computational burden involved in solving SHE equations that contain trigonometric terms.

In this study, a standalone solar array-connected multilevel inverter is proposed for low power single-phase applications in remote and rural locations. Unlike three-phase applications in which the triplen harmonics automatically cancel out, these harmonics constitute part of the total harmonic distortion (THD) in single-phase applications thereby making it more difficult to meet the maximum THD value of 5% specified IEEE 519-1992 and IEC61000-3-12.

2. STANDALONE PV-CONNECTED INVERTER

Sequel to the proliferation of high-speed semiconductor switches with high-power handling capability and advances made in PV cells technology that have resulted into improved conversion efficiency at reduced cost, standalone and grid-connected inverters have continued to garner interest. In cascaded H-bridge multilevel inverter with varying DC input voltage sources such as PV array-connected inverter, modulation control of the H-bridge switches or DC input voltage regulation with a DC-DC converter is used to ensure a constant fundamental voltage at the output of the inverter [9]. The narrow range of modulation index of single-phase multilevel inverter makes the first approach infeasible. Hence, the adopted approach in this study is the regulation of DC voltage with boost converter.

The proposed standalone PV-connected single-phase multilevel inverter comprises of an array of solar panels that convert the renewable and inexhaustible solar energy into electrical energy, a DC-DC boost converter with maximum power point tracking (MPPT), energy storage system such as batteries, ultracapacitors etc, a single-phase DC-AC multilevel inverter (MLI) and controllers that ensures high efficiency by mitigating the variation of the output voltage of the PV cells with irradiance and temperature. The structure of a PV-connected single-phase inverter is shown in Figure 1.

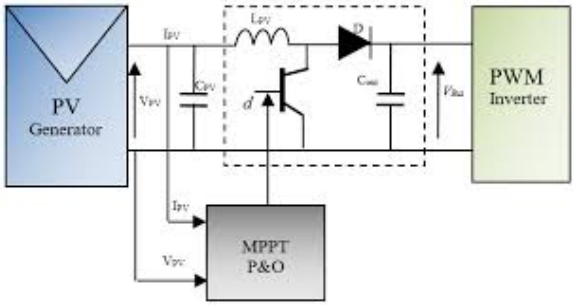

Figure1: Structure of a PV-connected single-phase inverter

A. Photovoltaic (PV) Cell Modeling

In solar PV generation system, solar energy is converted inti electrical energy using several PV cells that are connected in series and parallel [4]. A PV cell is basically a p-n junction that generates emf when illuminated by light. Using a single-diode model due to its accuracy and simplicity, a PV solar cell is modeled as shown in Figure 2.

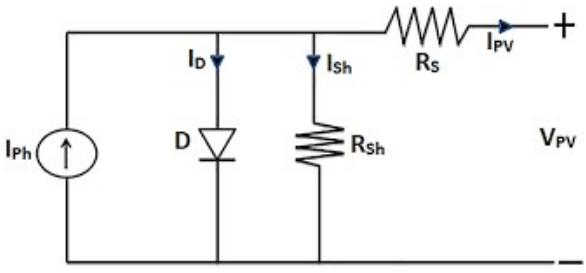

Figure 2: Single-diode model of PV module

The current-voltage relation of photovoltaic (PV) array is given by [10]

$$I_{PV} = n_p I_{SC} - n_p I_S \left[exp\left\{ \frac{q(V_{PV} + R_S I_{PV})}{AKTn_S} \right\} - 1 \right] \ldots$$
$$- n_p \frac{(V_{PV} + R_S I_{PV})}{n_S R_{Sh}} \quad (1)$$

Where

I_{PV} and V_{PV} are the output current and voltage of the PV array, respectively; R_S and R_{Sh} are the series and shunt resistances of the array, respectively; q is the electronic charge $(1.602 \times 10^{-19} C)$; k is the Boltzmann constant $(1.38 \times 10^{-23} J/K)$; T is the temperature (K); I_{SC} is the photocurrent; I_S is the reverse saturation current; A is the p-n junction ideality factor that is dimensionless; n_S and n_p are the number of PV cells connected in series and parallel, respectively.

As shown in Figure 3, PV cells exhibit nonlinear current-voltage and power-voltage characteristics that vary with temperature, irradiance and operating conditions of the PV cells [4].

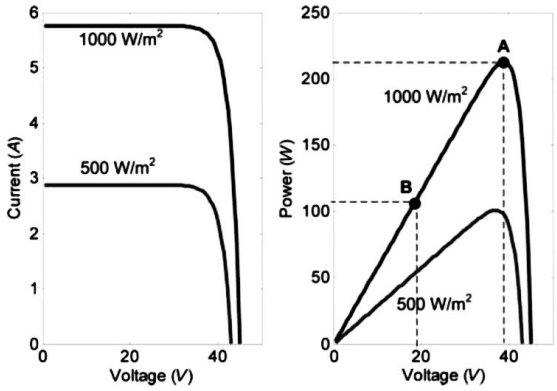

Figure 3: Typical I-V and P-V characteristics of PV module

The output power of the PV array, P_{PV} is given by

$$P_{PV} = I_{PV} V_{PV} \quad (2)$$

Maximum power is harnessed from PV module by tracking the maximum power point (MPP), which is the point of maximum efficiency of the PV array [4], [10], [11]. The output voltage at MPP is denoted by V_{MPP}. In order to ensure the operation of the PV array at MPP at all times, the value of V_{MPP} is continuously tracked using maximum power point tracking (MPPT) techniques such as adaptive neuro-fuzzy inference system (ANFIS), perturb and observe, hill climbing, adaptive hysteresis-band and incremental conductance algorithms [4], [11]. The adopted MPPT algorithm in this work is perturb and observe due to its simplicity and efficiency. Perturb and observe MPPT algorithm works by periodically perturbing the operating voltage by a fixed amount in a particular direction. If there is increase in power, perturbation continues in the direction. However, if power decreases, the direction of perturbation is reversed. Detailed explanation on the operating principle of perturb and observe MPPT algorithm can be found in [11].

B. DC-DC Boost Converter

Boost converter is a switch-mode DC-DC converter that steps up the level of input DC voltage to a specified value of DC output voltage by stepping down the value of the input current [12].

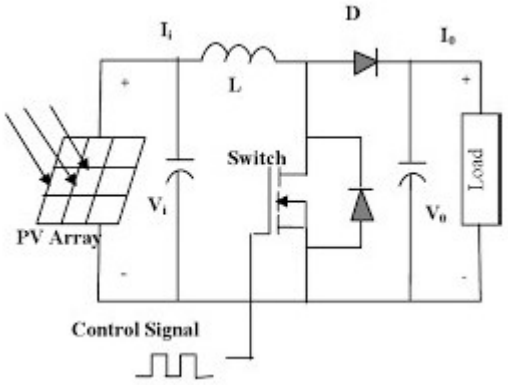

Figure 4. DC-DC boost converter with PV array

The output voltage and current of boost converter are given by (3) and (4), respectively [12].

$$V_o = \frac{V_{in}}{1-D} \quad (3)$$

$$I_o = I_{in}(1-D) \quad (4)$$

The values of inductance L, capacitance C and load resistance shown in Figure 4 are calculated with (5), (6) and (7), respectively as follows

$$L = \frac{V_{in}(V_o - V_{in})}{f_{sw} \times \Delta I \times V_o} \quad (5)$$

$$C = \frac{I_o(V_o - V_{in})}{f_{sw} \times \Delta V \times V_o} \quad (6)$$

$$Z_L = \frac{V_o}{I_o} \quad (7)$$

Where V_{in} is the input DC voltage, D is the duty cycle of the converter, ΔI is the ripple current, ΔV is the ripple voltage and f_{sw} is the switching frequency. By the rule of thumb,
ΔI = 5% of the input DC current
ΔV = 1% of the output DC voltage

C. Multilevel Inverter Topologies

The development of multilevel inverters stemmed from the step approximation of sinusoid [13]. There are basically three multilevel inverter topologies. These are Diode-Clamped Multilevel Inverter [14], Capacitor-Clamped Multilevel Inverter [15], and Cascaded H-bridge Multilevel Inverter with separate DC sources (SDCSs) [16]. Compared with the other topologies, cascaded H-bridge inverter has the advantages of least number of components requirement, modularity and circuit layout flexibility, which make it suitable for high-voltage and high-power applications.

The number of output voltage levels in a cascaded H-Bridge inverter is given by *m* =2s +1, where s is the number of H-bridges connected in cascade. Thus, 11-level cascaded H-bridge inverter is formed by connecting five single-phase H-bridge inverters in series as shown in Figure 1.

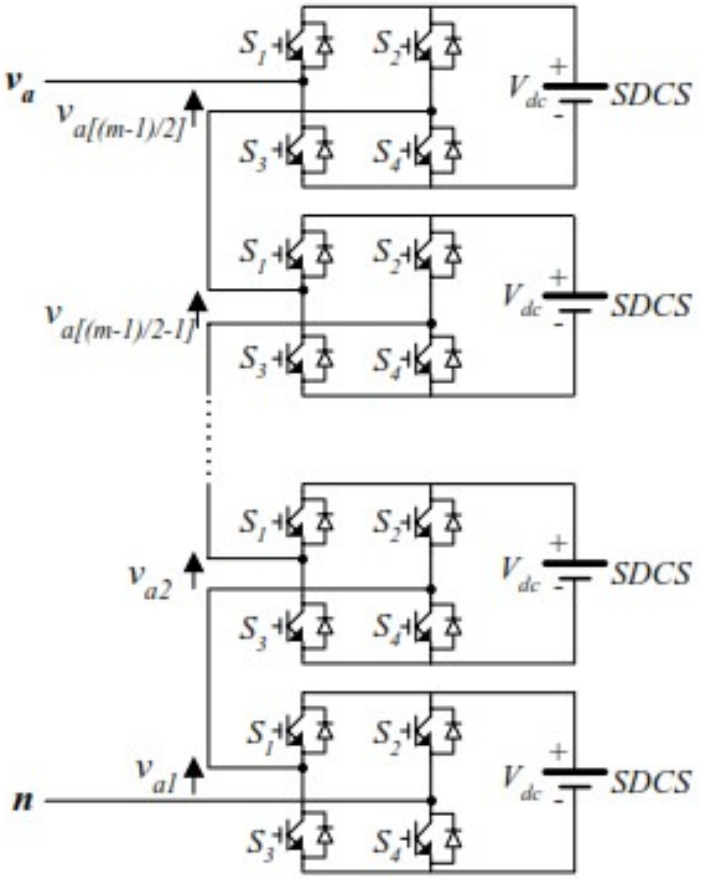

Figure 5. Single phase structure of an m-level CHB inverter.

By different combinations of the four switchesS_1, S_2, S_3, and S_4 shown in the Figure1, each H-bridge switch can generate a square wave voltage waveform with different duty cycle on the AC side. When switches S_1 and S_4 are turned on, $+V_{dc}$ is obtained while $-V_{dc}$ is obtained by turning on switches S_2 and S_3. The output voltage is zero when either S_1 andS_2, or S_3 and S_4 are turned on. The outputs of H-bridge switches are connected in series such that the synthesized AC voltage waveform is the summation of all voltages from the cascaded H-bridge cells [17].

D. SHE-PWM SWITCHING TECHNIQUES

The output voltage waveform of a single-phase 11-level inverter shown in Figure 6 is periodic with odd quarter-wave symmetry. Generally, any periodic waveform can be shown to be the superposition of a fundamental signal and a set of harmonic components [17].

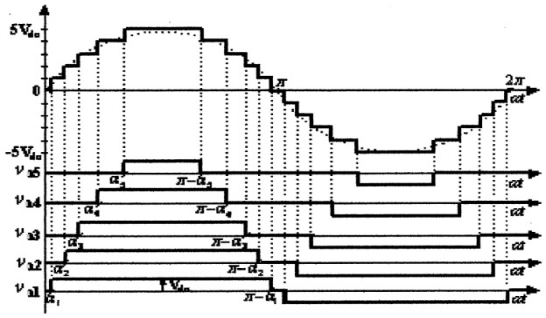

Figure 6. Voltage waveform of a single-phase 11-level inverter.

The Fourier series expansion of the waveform shown in Figure 6 is given by equation (8) [18].

$$V(\omega t) = V_n(\alpha)\, sin(n\omega t] \qquad (8)$$

Where

$V_n(\alpha) = \frac{4V_{dc}}{n\pi} \sum_{k=1}^{S} cos(n\alpha_k)$, for odd n (9)

$V_n(\alpha) = 0$, for even n (10)

From equations (8), (9) and (10),

$$v(\omega t) = \sum_{n=1,3,5..}^{\infty} \frac{4V_{dc}}{n\pi} (cos(n\alpha_1) + cos(n\alpha_2) + \ldots + cos(n\alpha_S))\, sinn\, \omega t) \qquad (11)$$

Subject to the switching angles constraint of $0 < \alpha_1 < \alpha_2 < \ldots \alpha_S \leq \pi/2$

Where *S* is the number of switching angles, which invariably is the same as the number of equations and *n* is the harmonic order. Generally, for *S* number of equations, one equation is used for the desired fundamental voltage V_1 while the remaining (S-1) equations are used to eliminate the predominant low order harmonics that dominate the total harmonic distortion (THD). The switching angles are chosen in such a way that the desired fundamental voltage V_1 is made equal to the first harmonic. Thus, equation (8) becomes

$$V(\omega t) = V_1\, sin(\omega t) \qquad (12)$$

From equation (11), the expression for the fundamental voltage V_1 in terms of the switching angles is given by

$$V_1 = \frac{4V_{dc}}{\pi} (cos(\alpha_1) + cos(\alpha_2) + \ldots + cos(\alpha_S)) \qquad (13)$$

The maximum fundamental voltage is obtained when all the switching angles are zero [19].

$$V_{1max} = \frac{4SV_{dc}}{\pi} \qquad (14)$$

The relation between the fundamental voltage and the maximum obtainable fundamental voltage V_{1max} is given by modulation index, m_i, which is defined as the ratio of the fundamental output voltage V_1 to the maximum obtainable fundamental voltage V_{1max}.

$$m_i = \frac{V_1}{V_{1max}} = \frac{\pi V_1}{4SV_{dc}} \quad (15)$$

The amplitude of the fundamental harmonic is

$$V_1 = m_i\left(\frac{4SV_{dc}}{\pi}\right) \quad (16)$$

For the development of an 11-level single-phase CHB inverter, five SDCSs are required. Unlike balanced three-phase system in which triplen harmonics in each phase automatically cancel out in line-to-line voltages, triplen harmonics have to be eliminated alongside the other odd harmonics in single-phase inverter. Thus, to eliminate the 3rd, 5th, 7th and 9th harmonics, five switching angles that satisfy the switching angles constraint of $0 < \alpha_1 < \alpha_2 < \ldots \alpha_5 \leq \pi/2$ are calculated from the following transcendental nonlinear equations known as SHE equations.

$$\begin{aligned}
&\frac{4V_{dc}}{\pi}(cos(\alpha_1) + cos(\alpha_2) + \ldots + cos(\alpha_5)) = V_1 \\
&cos(3\alpha_1) + cos(3\alpha_2) + \ldots + cos(3\alpha_5) = 0 \\
&cos(5\alpha_1) + cos(5\alpha_2) + \ldots + cos(5\alpha_5) = 0 \\
&cos(7\alpha_1) + cos(7\alpha_2) + \ldots + cos(7\alpha_5) = 0 \\
&cos(9\alpha_1) + cos(9\alpha_2) + \ldots + cos(9\alpha_5) = 0
\end{aligned} \quad (17)$$

Equation (16) in equation (17) yields:

$$\begin{aligned}
&cos(\alpha_1) + cos(\alpha_2) + \ldots + cos(\alpha_5) = 5_{mi} \\
&cos(3\alpha_1) + cos(3\alpha_2) + \ldots + cos(3\alpha_5) = 0 \\
&cos(5\alpha_1) + cos(5\alpha_2) + \ldots + cos(5\alpha_5) = 0 \\
&cos(7\alpha_1) + cos(7\alpha_2) + \ldots + cos(7\alpha_5) = 0 \\
&cos(9\alpha_1) + cos(9\alpha_2) + \ldots + cos(9\alpha_5) = 0
\end{aligned} \quad (18)$$

In its compact form, SHE equations give the relation between the modulation index and optimal switching angles.

$$F(\alpha) = B(m_i) \quad (19)$$

The Total Harmonic Distortion (THD) is computed as shown in equation (20):

$$THD = \sqrt{\sum_{i=3,5,7,9,\ldots}^{49}\left(\frac{V_i}{V_1}\right)^2} \quad (20)$$

3. NEWTON RAPHSON ITERATIVE METHOD

Newton-Raphson (NR) method is one of the fastest iterative methods for solving nonlinear equations [19]. This method begins with an arbitrarily chosen initial values and generally converges at the zero of a given system of nonlinear equations if the initial values are sufficiently close to the roots. The steps that are involved in the implementation of NR method for solving selective harmonic elimination (SHE) equations are shown in Figure 7:

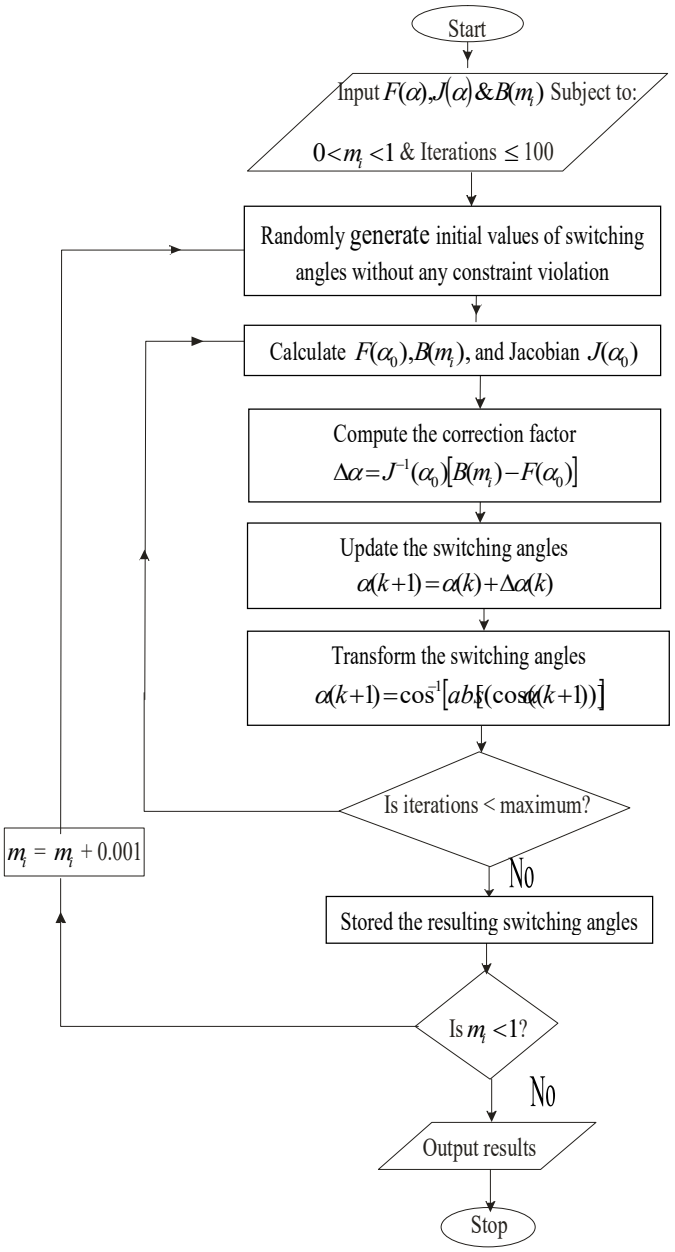

Figure 7. Flowchart of Newton Raphson algorithm for solving SHE equations.

4. IMPLEMENTATION

Using MATLAB software, a set of SHE equations shown in equation (18) was solved with Newton Raphson algorithm to eliminate 3rd, 5th, 7th, and 9th harmonics, which are the predominant lower order harmonics in an 11-level single-phase CHB inverter. The computations were carried out with a personal computer (1.7 GHz Intel Core i3 dual processor with 4GB Random Access Memory) running MATLAB R2021a on Windows 10 Pro. The modulation index, m_i was incremented in steps of 0.001 from 0 to 1 to compute the solutions.

In order to validate the computational results, an 11-level single-phase CHB inverter was modelled and simulated using SimPower System block set in MATLAB-SIMULINK. Each of the five H-Bridges in the 11-level single-phase CHB inverter requires a separate DC source (SDCS) of V_{dc} provided by the PV array-connected boost converter shown in Figure 12. Simulations were performed using the solution set with the least 49th order THD value of 6.51 % found at the modulation index m_i of 0.8, which is $[5.6773^o\ 16.4853^o\ 30.6968^o\ 42.0136^o\ 63.6953^o]$. From equation (15), DC link voltage (V_{dc}) of $63.87\ V\ (\approx 64\ V)$ is required to synthesize AC voltage of 230 V, 50 Hz at $m_i = 0.8$. The solar panel chosen for the implementation of this work is Sunny International Power SPM-250PB205 with the specifications shown in Table 1. The manufacturer's experimental I-V and P-V curves for a 1x4 PV array at the standard test conditions (STD) of 25^oC cell temperature and solar irradiance of $1000W/m^2$ are shown in Figure

Table 1: PV module and 1x4 PV array specification at STC

Parameter	PV Module	PV Array
Maximum Power (P_{max})	250.158 W	1 kW
Open circuit voltage (V_{oc})	43.4 V	43.4 V
Short circuit current (I_{sc})	7.8 A	31.2 A
Voltage at P_{max} (V_{mpp})	34.6 V	34.6 V
Current at P_{max} (I_{mpp})	7.23 A	28.92 A

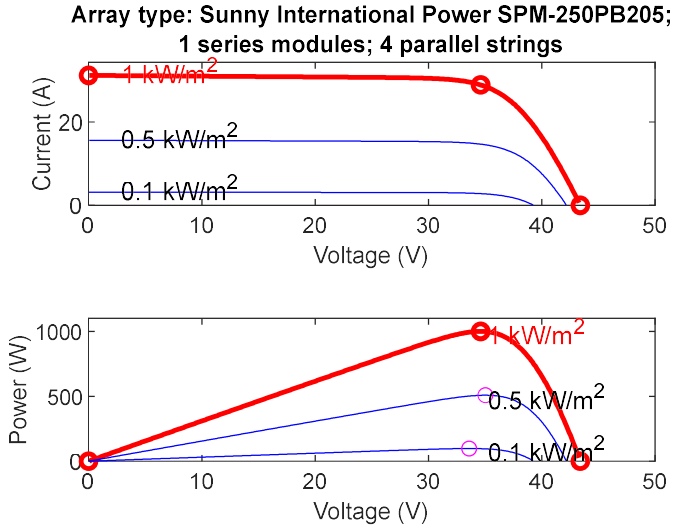

Figure 8. I-V and P-V characteristics of the chosen 1x4 PV array

The values of the boost converter parameters calculated with eqs 4-6 are shown in Table 2.

Table 2: Boost converter parameters

Parameter	Values
Input voltage (V_{in})	34.6 V
Input current (I_{in})	28.92 A
Inductance (L)	0.44 mH
Capacitance (C)	198.5 µF
Load resistance (R_L)	4.1 Ω
Switching frequency (f_{sw})	25 kHz
Duty cycle (D)	0.46

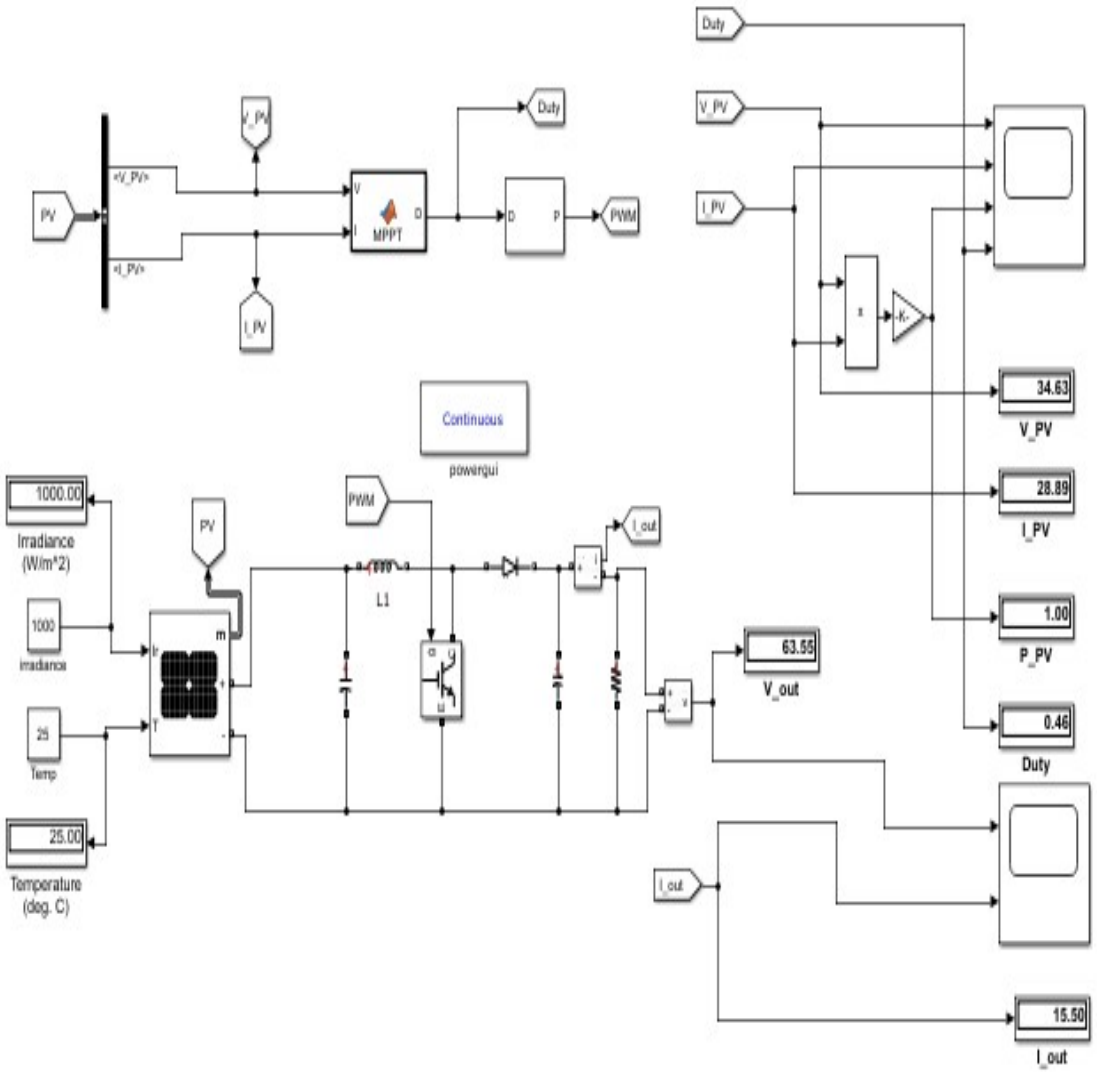

Figure 9. Model structure of the PV array-connected boost converter.

6. RESULTS

Figure 10 shows the plot of switching angles that minimize 3rd, 5th, 7th, and 9th harmonics in a single-phase 11-level inverter. It can be seen from Figure 10 that a single-phase 11-level inverter has a very narrow range of modulation index with feasible solution sets [0.643-0.686] and [0.8]. As shown in Figure 11, the solution set with the least 49th order THD value of 6.51% is found at the modulation index of 0.8. The plot of the 9th order THD shows that the selected harmonics are considerably eliminated for all the solution sets.

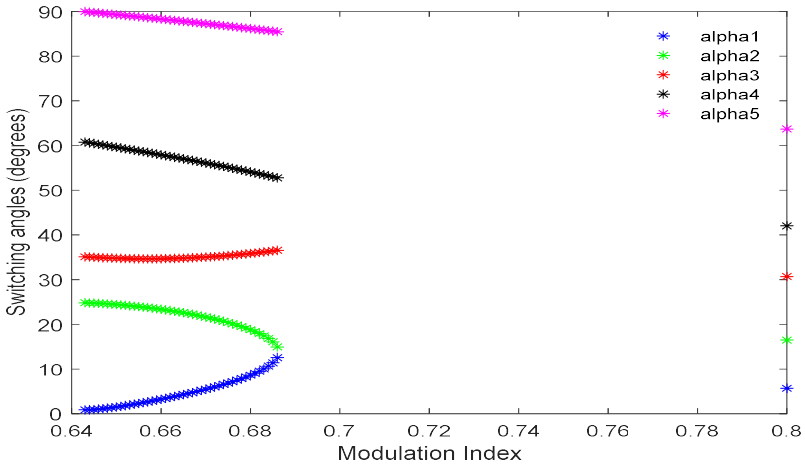

Figure 10. Plot of switching angles against modulation index for an 11-level single-phase inverter.

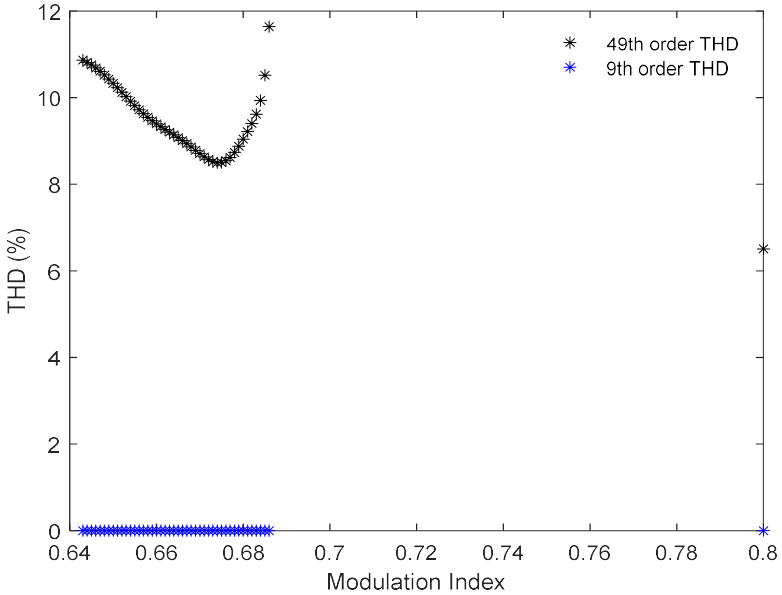

Figure 11. Plot of 9th and 49th order THD against modulation index for an 11-level single-phase inverter

Shown in Figure 12 are the plots of the input voltage, input current and output power of the PV array as well as duty cycle. The figure shows how the input voltage and input current of the PV array alongside the duty cycle are varied by the perturb and observe MPPT algorithm to ensure that the maximum power of 1 kW is delivered by each PV-connected boost converter.

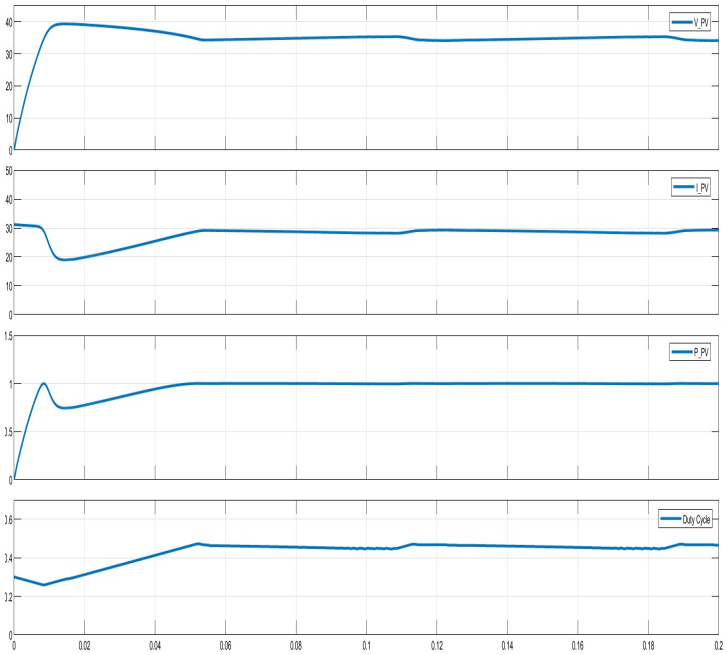

Figure 12. Plots of the perturb and observe MPPT algorithm-controlled input voltage, input current, output power and duty cycle.

As shown in Figure 13, the MPPT algorithm ensures that the output voltage and current of the PV-connected boost converter remain relatively constant at 64V and 15.61A, respectively.

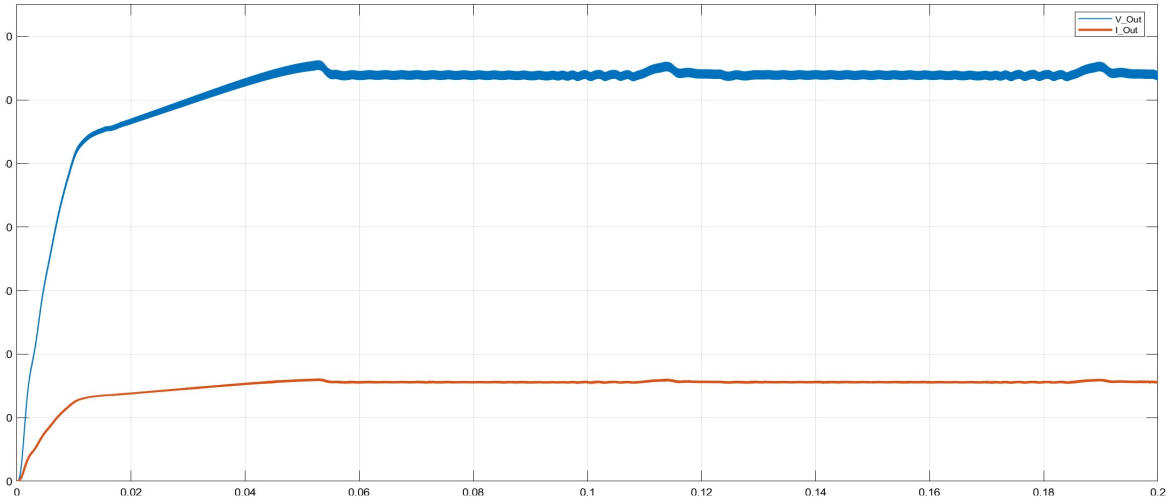

Figure 13. Plots of the output voltage and current of the PV-connected boost converter.

The viablity of the proposed PV-connected 11-level single-phase inverter has been demonstrated with simulations in MATLAB/SIMULIKNK. Figure 14 shows the output voltage waveform of the the inverter simulated at $m_i = 0.8, V_{dc} = 64\ V\ and\ freq = 50\ Hz$.

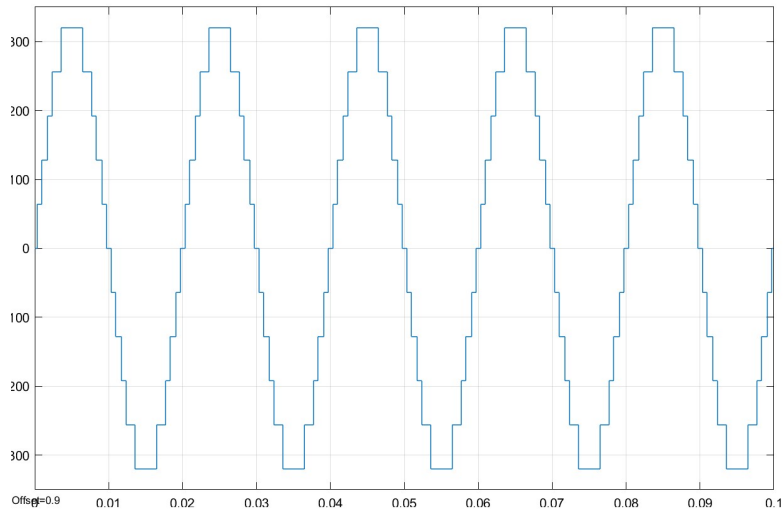

Figure 14. 11-level voltage waveform simulated at $m_i = 0.8, V_{dc} = 64\ V\ and\ freq = 50Hz$

Fast Fourier transform (FFT) analysis of the simulated phase voltage waveforms was done using the FFT block to show the harmonic spectrum of the synthesized AC voltage. Figure 15 shows the normalized FFT plot of the phase voltage waveform shown in Figure 14.

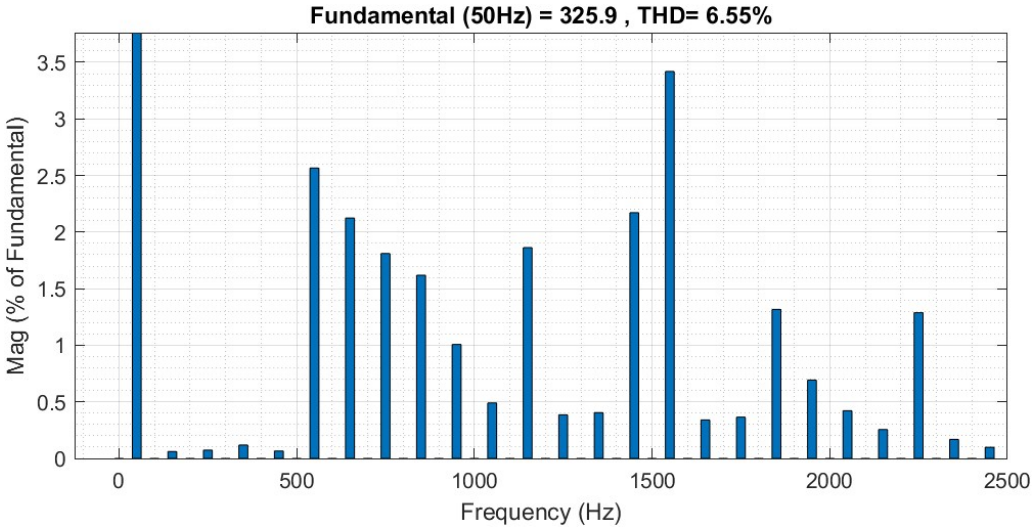

Figure 15. Normalized FFT plot of the 11-level voltage waveform at $m_i = 0.8$

The FFT analysis shows that all the harmonics up to 10th order are approximately zero, which corroborates the computational results. Table 3 shows the comparative study of the computational and simulation results for 49th order THD and amplitude of the fundamental voltage at $m_i = 0.8$.

Table 3: Comparison of computational and simulation results at $m_i = 0.8$

Parameter	Computational Result	Simulation Result
49th order THD	6.51%	6.55%
Peak value of fundamental voltage	325.27 V	325.9 V

Both results are in close agreement demonstrating the efficiency of the proposed model.

7. CONCLUSION

A PV-connected standalone single-phase 11-level inverter is presented for distributed power generation in remote and rural locations that are unconnected to the grid. To mitigate the variation of solar generated voltage with temperature and irradiance, DC-DC boost converter with perturb and observe MPPT algorithm has been successfully implemented for voltage regulation. The viability of the proposed PV array-connected multilevel inverter has been demonstrated with simulations in MATLAB/SIMULIKNK environment. Fast Fourier transform (FFT) of the simulated 11-level voltage waveform shows that the selected harmonics are eliminated as desired while THD is 6.55 %. Computational results have been corroborated with simulation results and both are in close agreement. Having eliminated the low order harmonics that are predominant and difficult to remove with filter due to their closeness in value with the fundamental voltage, higher order harmonics can be removed with lowpass LC filter.

REFERENCES

[1] J. A. Peças, "Integrating Distributed Generation into Electric Power Systems: A Review of Drivers, Challenges and Opportunities," Electric Power Systems Research, Volume 77, No. 9, pp. 1189-1203.

[2] S. Amamra, K. Meghriche, A. Cherifi and B. Francois, "Multilevel Inverter Topology for Renewable Energy Grid Integration," IEEE Transactions on Industrial Electronics, Vol. 64, Issue 11, Nov, 2017, pp. 1-10.

[3] P. Xu, X. Zhang, C. W. Zhang, R. X. Cao and L. Chang, "Study of Z-Source Inverter for Grid-Connected PV Systems," in Proc. 37th IEEE Power Electronics Specialist Conference (PESC ;06), Jun. 2006, pp. 1-5.

[4] J. Ekanayake, k. Liyanage, J. Wu, A. Yokohama andN. Jenkins, Smart Grid: Technology and Applications, First Edition 2012 Published by John Wiley and Sons Ltd.

[5] S. Daher, "Analysis, Design and Implementation of a High Efficiency Multilevel Converter for Renewable Energy Systems," Unpublished Ph. D thesis, University of Kassel, Germany, 2006.

[6] J. M. Vesapogu, J. M. Peddakotla and S. R. A. Kuppa, "Harmonic Analysis and FPGA Implementation of SHE Controlled Three-Phase CHB 11-Level Inverter in MV Drives using Deterministic and Stochastic Optimization Techniques" Springer Plus 2:237, 2013.

[7] S. Khomfoi and L. M Tolbert, Chapter31. Multilevel Power Converters. The University of Tennessee. pp.31-1 to 31-50.

[8] J. Rodríguez, J. Lai, and F. Peng, "Multilevel inverters: a survey of topologies, controls and applications," *IEEE Transactions on Industry Applications*, vol. 49, no. 4, pp. 724-738, Aug. 2002.

[9] F. Filho, L. M. Tolbert, Y. Cao and B. Ozpineci, "Real-Time Selective Harmonic Minimization for Multilevel Inverters Connected to Solar Panels using Artificial Neural Network Angle Generation," *IEEE Transactions on Industry Applications*, vol. 47, Issue 5, pp. 2117-2124, Sept-Oct. 2011.

[10] N. A. Ahmed, M. Miyatake and A. K. Al-Othman, "Power fluctuation suppression of stand-alone hybrid generation combining photovoltaic/wind turbine and fuel cell systems" Energy Conversion and Management, 49 (10), pp. 2711-2719, May 2008.
[11] S. Sengar, "Maximum Power Point Tracking Algorithms for Photovoltaic System: A Review," International Review of Applied Engineering Research, vol. 4, no. 2, pp. 147-154, 2014.
[12] M. H. Rashid, Power Electronics Circuits, Devices and Applications, Second Edition 1993 Published by Prentice-Hall, Inc.
[13] R. H. Baker and L. H. Bannister, "Electric power converter," U.S. Patent 3867643, Feb. 1975.
[14] A. Nabae, I. Takahashi and H. Akagi, "A new neutral-point clamped PWM inverter,"*IEEE Trans. Ind. Applicat.*, vol. IA-17, Sept./Oct. 1981, pp. 518–523.
[15] T. A. Meynard and H. Foch, "Multi-level conversion: High voltage choppers and voltage- source inverters," in *Proc. IEEE-PESC*, 1992, pp. 397–403.
[16] P. Hammond, "A new approach to enhance power quality for medium voltage ac drives," *IEEE Trans. Ind. Applicat.*, vol. 33, pp. 202–208, Jan./Feb. 1997.
[17] J. Chiasson, L. M. Tolbert, K. McKenzie, and Z. Du, "Elimination of Harmonics in a Multilevel Converter using the Theory of Symmetric Polynomial and Resultant," Proceedings of the 42nd IEEE Conference on Decision and Control, Dec. 2005, pp. 216-223.
[18] S. Sirisukprasert, J. S. Lai, and T. H, Liu, "Optimum Harmonic with a Wide Range of Modulation Indixes for Multilevel Converters," IEEE Transaction on Industrial Electronics, Vol. 49, no; 4, August 2002, pp. 875-881.
[19] J. Kumar, B. Das, and P. Agarwal, "Selective Harmonic Elimination Technique for Multilevel Inverter," 15th National Power System Conference (NPSC), IIT Bombay, 2008, pp. 608-613. Engineering, Vol. 3, Issue 3, pp. 8031-8040, March 2014.